# Measurement of $\Gamma_{ee} \times \mathcal{B}_{\mu\mu}$ for $\psi(2S)$ meson with KEDR detector

**Andrey Sukharev for the KEDR Collaboration**

Budker Institute of Nuclear Physics, Novosibirsk, Russia

A.M.Suharev@inp.nsk.su

**Abstract**

*Based on the nine data sets taken with the KEDR detector since 2004 in charmonia region, we report $\Gamma_{ee} \times \mathcal{B}_{\mu\mu} = 19.5 \pm 0.3 \pm 0.4$ eV for $\psi(2S)$ meson. The total luminosity accounted for is more than 6.5 pb$^{-1}$, corresponding to about $4 \times 10^6$ $\psi(2S)$.*
*There were several scans of the resonance allowing us to know the collider energy spread and several runs where the data was taken at the $\psi(2S)$ peak and slightly below it. The Particle Data Group does not mention any direct measurement of this quantity yet. Instead, many $\psi(2S)$ parameters, including partial widths and branching ratios, are obtained using a complicated simultaneous fit of results of various experiments.*

## 1. VEPP-4M collider and KEDR detector

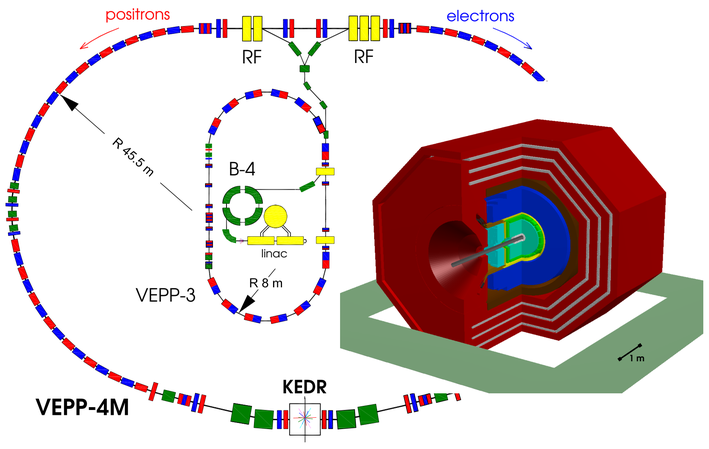


**Figure 1:** *VEPP-4M/KEDR complex with the injector facility.*

VEPP-4M parameters at $\psi(2S)$:

| | |
|---|---|
| Peak luminosity | $\sim 2 \times 10^{30}\,\text{cm}^{-2}\text{s}^{-1}$ |
| Energy measurement precision | $6 \cdot 10^{-6}$ ($\simeq$20 keV) |

## 2. Theoretical $e^+e^- \to \ell^+\ell^-$ cross section

The analytic expressions for the cross section of the process $e^+e^- \to \ell^+\ell^-$ with radiative corrections taken into account in the soft photon approximation were first derived by Ya. A. Azimov *et al.*, JETP Lett. **21**, 172 (1975). With some up-to-date modifications one obtains in the vicinity of a narrow resonance:

$$\left(\frac{d\sigma}{d\Omega}\right)^{ee\to\mu\mu} \approx \frac{3}{4M^2}(1+\delta_{\text{sf}})\left(1+\cos^2\theta\right) \times \left\{\frac{3\Gamma_{ee}\Gamma_{\mu\mu}}{\Gamma M}\text{Im}f - \frac{2\alpha\sqrt{\Gamma_{ee}\Gamma_{\mu\mu}}}{M}\text{Re}\frac{f}{1-\Pi_0}\right\} + \left(\frac{d\sigma}{d\Omega}\right)^{\mu\mu}_{\text{QED}},$$

where a correction $\delta_{\text{sf}}$ follows from the structure function approach of E. A. Kuraev and V. S. Fadin, Sov. J. Nucl. Phys. **41**, 466 (1985).

$$f = \frac{\pi\beta}{\sin\pi\beta}\left(\frac{M/2}{-W+M-i\Gamma/2}\right)^{1-\beta}, \quad \beta = \frac{4\alpha}{\pi}\left(\ln\frac{W}{m_e} - \frac{1}{2}\right)$$

Theoretical cross section has to be convoluted with the collider's energy spread distribution, which is taken as Gaussian.

## 3. Data taking and event selection

Several data sets in the $\psi(2S)$ region were recorded with the KEDR detector since 2004 (Table 1).

**Table 1:** *KEDR $\psi(2S)$ data sets*

| Data set | Period | $L_{sum}$, nb$^{-1}$ | $\sigma_W$, MeV |
|---|---|---|---|
| peak/cont. 1 | begin 2005 | 358 | 1.08 |
| peak/cont. 2 | autumn 2005 | 222 | 0.99 |
| scan 1 | spring 2006 | 255 | 0.99 |
| peak/cont. 3 | spring 2006 | 631 | 0.99 |
| peak/cont. 4 | autumn 2006 | 701 | 0.99 |
| peak/cont. 5 | autumn 2007 | 1081 | 1.01 |
| scan 2 | end 2007 | 967 | 1.01 |
| scan 3 | summer 2010 | 379 | 1.00 |
| scan 4 | end 2010 | 2005 | 0.98 |

Two modes of data taking were employed. In the scan mode, the experimental data were collected at minimum five energy points around the $\psi(2S)$ resonance — near the $\psi(2S)$ cross section peak, at its slopes, and in the continuum slightly below and above the resonance. In the peak/continuum mode, only two energy points were recorded — at the peak and slightly below it.

A data sample considered in this analysis corresponds to a total integrated luminosity of more than 6.5 pb$^{-1}$ or about $4 \times 10^6$ $\psi(2S)$ decays.

The collider energy spread $\sigma_W$ was determined in scans using $e^+e^- \to$ hadrons channel.

The following event selection criteria for $e^+e^-$ and $\mu^+\mu^-$ were used:

1. Two-prong central event, opposite charges, acollinearity on $\theta$ and $\varphi$ less than 28°, energy deposit on each track less than 700 MeV for muons or greater than 800 MeV for electrons.
2. $40° < \theta < 140°$ for $e^+e^-$, $50° < \theta < 130°$ for $\mu^+\mu^-$.
3. Not more than one extra cluster, with energy less than 160 MeV.
4. For muons — confirmation from muon system for both tracks, anti-cosmic time-of-flight veto $|t \times \sin\theta - T_0| \leqslant 3\sigma_{\text{tof}}$.

## 4. ToF efficiency

Due to digitization electronics problem, there is a time measurement inefficiency in the Time of Flight system (not affecting the trigger). The anti-cosmic cut efficiency is not accounted in simulation and has to be measured separately.

The efficiency was determined with two independent methods:

1. Using cascade decay $\psi(2S) \to J/\psi\pi\pi, J/\psi \to \mu^+\mu^-$.
2. Measuring efficiency for one muon putting the ToF cut on another and subtracting the residual cosmic background statistically. The total efficiency $\varepsilon = \varepsilon_+\varepsilon_-$, providing $\varepsilon_+$ and $\varepsilon_-$ are uncorrelated (checked with $J/\psi \to e^+e^-$).

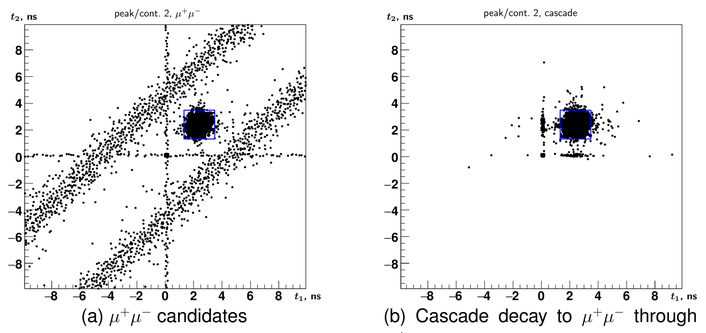


(a) $\mu^+\mu^-$ candidates (b) Cascade decay to $\mu^+\mu^-$ through $J/\psi\pi\pi$.

**Figure 2:** *Time-of-flight distribution example for $\mu^+\mu^-$ candidates. The cut is shown with a square. Events with lost time are located at $t_{1,2} = 0$. Slant stripes correspond to cosmic events.*

The ToF cut efficiency varies from 79% to 87% with data set.

## 5. Data analysis

A combined fit of $e^+e^-$ and muon data was performed. It allows to determine $\Gamma_{ee} \times \mathcal{B}_{\mu\mu}$ and $\Gamma_{ee} \times \mathcal{B}_{ee}$ as well as the luminosity by bhabha and $\mu^+\mu^-$ scattering. To extract luminosity, the set of $e^+e^-$ events was divided into four equal angular intervals of the polar angle $\theta$ from $40°$ to $140°$. At the $i$-th energy $W_i$ and the $j$-th angular interval $\theta_j$, the expected number of $e^+e^- \to e^+e^-$ events was parametrized as

$$N^{\text{ex}}_{e^+e^-}(W_i,\theta_j) = \mathcal{L}_i \cdot \sigma^{\text{ex}}_{ee}(W_i,\theta_j),$$
$$\sigma^{\text{ex}}_{ee}(W_i,\theta_j) = \sigma^{\text{th}}_{\text{res}}(W_i,\theta_j)\cdot\varepsilon_{\text{res}}(\theta_j)|_i + \sigma^{\text{th}}_{\text{int}}(W_i,\theta_j)\cdot\varepsilon_{\text{int}}(\theta_j)|_i + \sigma^{\text{sim}}_{\text{cont}}(W_i,\theta_j)\cdot\varepsilon_{\text{cont}}(\theta_j)|_i + \sigma^{\text{ex}}_{\text{bg}}(W_i,\theta_j),$$

where $\mathcal{L}_i$ — total luminosity at $W_i$, $\sigma^{\text{th}}$ — theoretical cross sections for elastic scattering, resonance and interference, $\varepsilon(\theta_j)|_i$ — detection efficiencies for the $j$-th angular interval obtained with simulation. The last term of the sum is the expected contribution of background processes. Each contribution has its own angular distribution and thus its own registration efficiency.

Since there are no angular $\theta$ bins for $\mu^+\mu^-$, the expected number of events at energy $W_i$ is just:

$$N^{\text{ex}}_{\mu^+\mu^-}(W_i) = \mathcal{L}_i \cdot \sigma^{\text{ex}}_{\mu\mu}(W_i),$$
$$\sigma^{\text{ex}}_{\mu\mu}(W_i) = \varepsilon^{\text{obs}}_{\text{tof}}|_i \times \Big((\sigma^{\text{th}}_{\text{res}}(W_i) + \sigma^{\text{th}}_{\text{int}}(W_i))\cdot\varepsilon_{\text{res}}|_i + \sigma^{\text{sim}}_{\text{cont}}\cdot\varepsilon_{\text{cont}}|_i + \sigma^{\text{ex}}_{\text{bg}}(W_i)\Big),$$

which also includes the measured ToF efficiency $\varepsilon^{\text{obs}}_{\text{tof}}$. The resonance and interference for muons have equal angular distributions and thus equal efficiencies.

Continuum cross sections $\sigma^{\text{sim}}_{\text{cont}}$ for both $e^+e^-$ and $\mu^+\mu^-$ are calculated in the simulation program (the MCGPJ generator) which also accounts for the radiative corrections.

The expected background contribution is a sum of the background decay modes:

$$\sigma^{\text{ex}}_{\text{bg}}(W_i) = \sum_m \sigma^{\text{th}}_m(W_i)\varepsilon_m|_i, \qquad (1)$$

where $\varepsilon_m$ — mode $m$ efficiency (individually for each $\theta$ bin in the $e^+e^-$ case), and its theoretical cross section $\sigma^{\text{th}}_m(W)$ is calculated using the PDG mode branching ratio $\mathcal{B}_m$. $\varepsilon_m$ was determined using simulation. Total background correction varies with data set from about 4% to 8%, dominating part coming from cascade decays $\psi(2S) \to J/\psi\pi\pi, J/\psi \to \ell^+\ell^-$ and from radiative decays $\psi(2S) \to \gamma\chi_c$.

The combined fit free parameters were $\Gamma_{ee} \times \mathcal{B}_{\mu\mu}$ and $\Gamma_{ee} \times \mathcal{B}_{ee}$.

## 6. Systematic uncertainties

The data sets are considered as semi-independent experiments with partially correlated systematic errors. To obtain the average result, each measurement weight accounts for its statistical error and its uncorrelated part of systematic errors. In most cases it is assumed that the correlated part of systematic uncertainty corresponds to the minimal uncertainty in data sets for a given uncertainty source.

**Table 2:** *Main sources of systematic uncertainties and their relative contributions, %.*

| | Systematic uncertainty source | p/c 1 | p/c 2 | sc. 1 | p/c 3 | p/c 4 | p/c 5 | sc. 2 | sc. 3 | sc. 4 | $\sigma^{\text{corr}}_{\text{syst}}$ |
|---|---|---|---|---|---|---|---|---|---|---|---|
| 1 | Energy spread | 2.3 | 2.7 | 0.8 | 2.3 | 2.4 | 2.8 | 1.1 | 2.8 | 1.9 | 0 |
| 2 | Fixed values of $M_{\psi(2S)}$, $\Gamma_{\psi(2S)}$ | 0.7 | 0.6 | 0.1 | 0.3 | 0.7 | 0.6 | 0.5 | 0.2 | 0.9 | 0.1 |
| 3 | Energy measurement | 3.1 | 0.6 | $< 0.1$ | 1.7 | 0.3 | 0.5 | 0.2 | 1.6 | 2.7 | $< 0.1$ |
| 4 | Bhabha simulation | 0.7 | 0.2 | 0.2 | 0.2 | 0.3 | 0.4 | 0.2 | 0.4 | 0.2 | 0.2 |
| 5 | $\mu^+\mu^-$ scattering simulation | 0.2 | 0.2 | 0.3 | 0.2 | 0.2 | 0.2 | 0.3 | 0.2 | 0.2 | 0.2 |
| 6 | Collinearity cuts | 0.4 | 1.4 | 1.0 | 1.6 | 0.9 | 0.6 | 0.9 | 4.3 | 1.8 | 0.4 |
| 7 | $e^+e^-$ polar angle range | 3.7 | 1.0 | 2.1 | 1.0 | 2.0 | 0.7 | 2.5 | 3.5 | 2.0 | 0.7 |
| 8 | Charge determination | 0.2 | 0.3 | 0.6 | 0.3 | 0.1 | 1.4 | 0.3 | 0.5 | 0.8 | 0.1 |
| 9 | Extra energy deposit cut | 1.3 | 0.5 | 1.9 | 0.3 | 1.5 | 0.9 | 2.6 | 1.4 | 1.7 | 0.3 |
| 10 | Muon system cut | 0.7 | 1.5 | 0.1 | 0.3 | 0.2 | 1.4 | 0.8 | 0.9 | 1.8 | 0 |
| 11 | ABG thresholds | 0.1 | 0.8 | 0.6 | 0.3 | 0.2 | — | — | — | — | 0.1 |
| 12 | Calo trigger thresholds | $< 0.1$ | 0.1 | 0.3 | 0.1 | $< 0.1$ | 0.4 | 0.5 | 0.2 | 0.1 | $< 0.1$ |
| 13 | RND trigger application | 0.4 | 0.5 | 0.2 | 0.2 | $< 0.1$ | 0.2 | 0.1 | 0.6 | 0.1 | $< 0.1$ |
| 14 | FSR accounting | 0.4 | 0.4 | 0.4 | 0.4 | 0.4 | 0.4 | 0.4 | 0.4 | 0.4 | 0.4 |
| 15 | $e^+e^-$ events $\theta$ binning | 0.6 | 0.1 | 0.4 | 0.2 | 0.2 | 0.2 | 0.3 | 0.4 | 0.1 | 0.1 |
| 16 | ToF measurement efficiency | 1.9 | 0.7 | 1.6 | 0.9 | 0.8 | 0.7 | 1.2 | 3.7 | 1.8 | 0.7 |
| 17 | Trigger efficiency | 0.9 | $< 0.1$ | 0.2 | 0.1 | 0.1 | 0.1 | 0.2 | 0.1 | 0.1 | $< 0.1$ |
| 18 | Theoretical accuracy | 0.1 | 0.1 | 0.1 | 0.1 | 0.1 | 0.1 | 0.1 | 0.1 | 0.1 | 0.1 |
| | Sum in quadrature | 6.1 | 3.9 | 3.7 | 3.6 | 3.8 | 3.8 | 4.2 | 7.7 | 5.4 | 1.2 |

## 7. Result

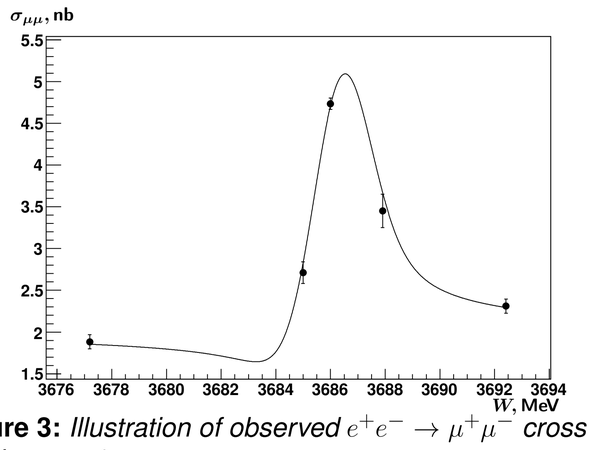


**Figure 3:** *Illustration of observed $e^+e^- \to \mu^+\mu^-$ cross section in scan 4.*

Averaging over nine data sets, we obtain the result $\Gamma_{ee} \times \mathcal{B}_{\mu\mu} = 19.5 \pm 0.3 \pm 0.4$ eV. The Particle Data Group does not mention any direct measurement of this quantity yet. Our result is compatible with the "world average" $\Gamma_{ee} \times \mathcal{B}_{\mu\mu} = 18.2 \pm 2.2$ eV calculated using $\Gamma_{ee}$ and $\mathcal{B}_{\mu\mu}$ from PDG and has better accuracy.

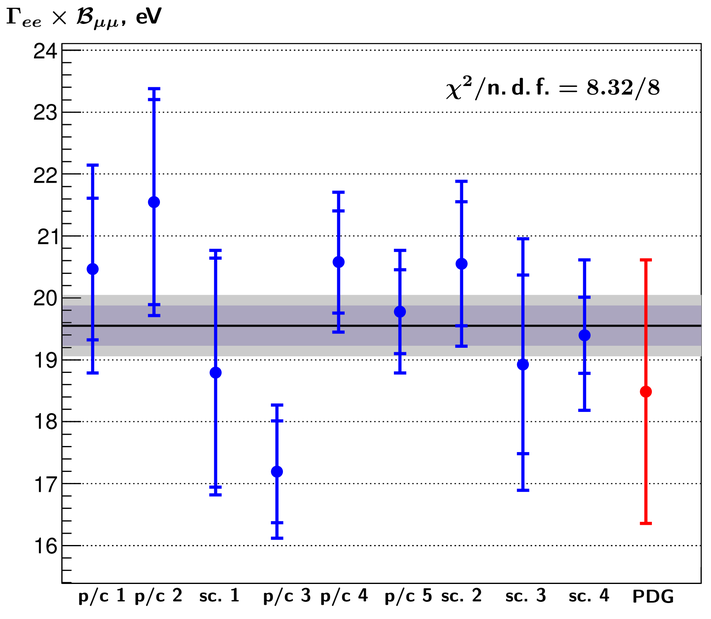


**Figure 4:** *$\Gamma_{ee} \times \mathcal{B}_{\mu\mu}$ measurements. Blue are KEDR measurements, red is product of PDG's $\Gamma_{ee}$ and $\mathcal{B}_{\mu^+\mu^-}$. KEDR result is shown with horizontal line and gray error bars. Statistical and total errors are shown for KEDR values.*